Journal of Ovarian Research

RESEARCH

Open Access

Reverse-engineering the FLT3-PI3K/AKT axis to enhance TILs function and improve prognosis in ovarian and cervical cancers

Feng Hao[1†], Zhang Yan[2†], Luo Shen[1], Wang Hui[1], Qiu Ling[1], Yang Xiaoyu[3*] and Jiang Hua[1*]

Abstract

Background Ovarian cancers (OC) and cervical cancers (CC) have poor survival rates. Tumor-infiltrating lymphocytes (TILs) play a pivotal role in prognosis, but shared immune mechanisms remain elusive.

Methods We integrated single-cell RNA sequencing (scRNA-seq) and spatial transcriptomics (ST) to explore immune regulation in OC and CC, focusing on the PI3K/AKT pathway and FLT3 as key modulators. Seurat and Harmony were employed for batch correction and dimensionality reduction. FLT3 expression was mapped with spatial data from 10×Genomics.

Results FLT3, identified as a regulator through the PI3K/AKT pathway, showed positive correlations with T cells, NK cells, and B cells. FLT3-high regions exhibited increased immune infiltration, particularly in CC, enhancing survival outcomes.

Conclusion This study provides the first spatially resolved evidence of FLT3's immune-modulatory role in OC and CC, positioning it as a promising immunotherapeutic target. FLT3-targeted strategies may offer new options for patients resistant to conventional therapies.

Keywords FLT3, PI3K/AKT pathway, Tumor-infiltrating lymphocytes (TILs), Ovarian cancer, Cervical cancer, Spatial transcriptomics

Introduction

Ovarian cancer (OC) and cervical cancer (CC) are two of the deadliest malignancies affecting women globally, with five-year survival rates as low as 30–40% [1]. Developing effective treatment strategies is essential to improve patient outcomes.

Emerging evidence highlights that tumor progression is driven not only by cancer cells but also by the tumor microenvironment (TME) [2–4], which consists of cancer cells, immune cells, fibroblasts, endothelial cells, and signaling molecules [5, 6]. The TME plays a central role in promoting tumor growth, invasion, and metastasis [7, 8].

Among these components, tumor-infiltrating lymphocytes (TILs) are particularly important for orchestrating the anti-tumor immune response and have been

†Feng Hao and Zhang Yan contributed equally to this work.

*Correspondence:
Yang Xiaoyu
Ehbh_yangxy@163.com
Jiang Hua
jianghua@fudan.edu.cn
[1] Department of Gynecology, Obstetrics and Gynecology Hospital of Fudan University, #128 Shenyang Road, Shanghai 200090, People's Republic of China
[2] Department of Cervical, Xiamen Women and Children's Healthcare Hospital, Women's and Children's Hospital of Xiamen University, #10 Zhenhai Road, Xiamen 361000, People's Republic of China
[3] HK International Regenerative Centre, MIRAMAR TWR 132 NATHAN RD Tsim Sha Tsui, Hong Kong Special Administrative Region, China

© The Author(s) 2025. **Open Access** This article is licensed under a Creative Commons Attribution-NonCommercial-NoDerivatives 4.0 International License, which permits any non-commercial use, sharing, distribution and reproduction in any medium or format, as long as you give appropriate credit to the original author(s) and the source, provide a link to the Creative Commons licence, and indicate if you modified the licensed material. You do not have permission under this licence to share adapted material derived from this article or parts of it. The images or other third party material in this article are included in the article's Creative Commons licence, unless indicated otherwise in a credit line to the material. If material is not included in the article's Creative Commons licence and your intended use is not permitted by statutory regulation or exceeds the permitted use, you will need to obtain permission directly from the copyright holder. To view a copy of this licence, visit http://creativecommons.org/licenses/by-nc-nd/4.0/.

associated with improved outcomes in immunotherapy [8, 9].TILs demonstrate clinical efficacy across various solid tumors, including triple-negative breast cancer [10], melanoma [11], lung cancer [12], ladder cancer [13], renal cell carcinoma [14], penile cancer [15], sarcoma [16], glioma [17], and pancreatic cancer [18] as well as ovarian [19, 20] and cervical cancers [21, 22]. Their success in clinical trials highlights their potential as both prognostic markers and therapeutic agents.

Given the therapeutic relevance of TILs in OC and CC, we hypothesize that shared signaling pathways regulate their immune activity, mediated by common regulatory genes that may serve as prognostic markers and therapeutic targets. To explore these mechanisms, we integrate single-cell RNA sequencing (scRNA-seq) and spatial transcriptomics (ST) data, leveraging these advanced technologies to uncover molecular pathways and spatial dynamics of immune responses. We began by analyzing T cells, the predominant immune cell population within TILs, to identify shared differentially expressed genes (DEGs) between OC and CC. Through pathway enrichment analysis, we uncovered that the PI3K/AKT signaling pathway—a critical regulator of immune cell activity and apoptosis—is significantly enriched in the shared DEGs. Focusing on this pathway, we performed prognostic and immune cell correlation analyses, which highlighted FLT3 as a key immune regulatory gene. FLT3 was found to correlate strongly with TILs activity, suggesting its potential role in enhancing immune responses through the PI3K/AKT pathway. To further validate these findings, we leveraged spatial transcriptomics data to analyze the spatial expression patterns of FLT3 and its co-localization with immune cells within the tumor microenvironment. This spatial analysis confirmed the association of FLT3 with immune cell infiltration and provided insights into its immune-modulatory functions within the tumor architecture. Through this integrative workflow (Fig. 1), we aim to identify shared regulatory genes and pathways, such as FLT3 and the PI3K/AKT signaling pathway, that could serve as actionable therapeutic strategies for ovarian and cervical cancers.

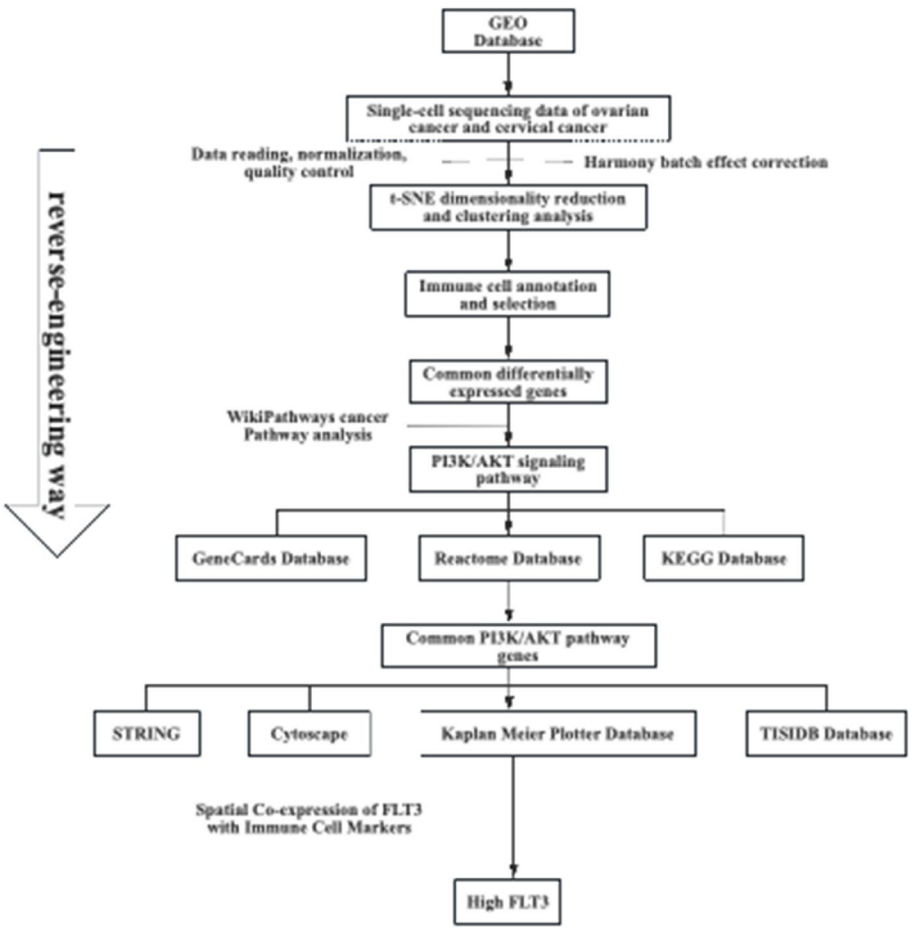

Fig.1 Flowchart of this study

Materials and methods

Identification of common immune-related signaling pathways in ovarian and cervical cancers

Data source and selection

To identify shared immune-related pathways between ovarian and cervical cancers, we analyzed publicly available single-cell RNA sequencing (scRNA-seq) datasets from the Gene Expression Omnibus (GEO) database (https://www.ncbi.nlm.nih.gov/geo/). The ovarian cancer cohort included seven high-grade serous ovarian carcinoma (HGSOC) samples and five normal ovarian tissue samples (GSE184880), while the cervical cancer cohort comprised three squamous cell carcinoma (SCC) samples and four normal cervical tissue samples (GSE197461&GSE208653). All datasets were generated using the Illumina NovaSeq 6000 platform (GPL24676) and provided in 10X Genomics format, ensuring compatibility with the Seurat package for downstream analysis. The overall workflow, including data acquisition, preprocessing, quality control, integration, and downstream analysis, is summarized in Supplementary Fig. 1.

Data preprocessing, quality control, and integration

We utilized Seurat for scRNA-seq data processing and Harmony to correct batch effects across datasets. Mitochondrial gene proportions were calculated using the PercentageFeatureSet function, and quality metrics such as gene detection counts, total RNA counts, and mitochondrial content were visualized to assess data quality. Standard quality control and cell filtering steps typically include identifying and excluding empty droplets, multiplets, and cells with abnormally high mitochondrial gene expression, which often indicate cell lysis [23]. To ensure the reliability and accuracy of downstream analyses, we applied the following stringent criteria: cells expressing fewer than 200 genes or more than 9,000 genes were excluded, as were cells with over 25% mitochondrial content. These thresholds were chosen to maintain a balance between eliminating low-quality cells and retaining sufficient data for robust analysis. Normalization was performed using the LogNormalize method, and the top 2,000 highly variable genes (HVGs) were identified with the FindVariableFeatures function for downstream clustering [24].

Differential gene expression analysis and annotation

To minimize technical variability, we employed the Harmony algorithm for data integration. Dimensionality reduction was performed using PCA, followed by t-SNE for clustering and visualizing transcriptional heterogeneity. The use of PCA prior to t-SNE emphasizes the primary structural features of the data while reducing noise, enabling more effective t-SNE visualizations that reveal distinct clustering patterns and relationships between cells. Immune cell annotation was conducted using canonical markers: CD3D, CD3E, and CD3G for T cells [25], CD19 for B cells [26], and FCGR3A, FCGR3B, and NCAM1 for NK cells [27]. Differential expression analysis was performed using the FindMarkers function from the Seurat package to compare gene expression levels in T cell populations between tumor and normal samples, identifying differentially expressed genes (DEGs). The Wilcoxon rank-sum test was used to evaluate the expression levels of each gene between the two groups, and an adjusted p-value threshold of < 0.05 was applied to ensure statistical significance. Shared immune-related DEGs were identified using a Venn diagram tool (http://bioinformatics.psb.ugent.be/webtools/Venn/) and further analyzed for pathway enrichment using WebGestalt (http://www.webgestalt.org/).

Clinical correlation analysis of PI3K/AKT pathway in ovarian and cervical cancers

Bioinformatics analysis of PI3K/AKT pathway-related genes

We identified PI3K/AKT pathway-related genes using three major bioinformatics databases: GeneCards, Reactome, and KEGG. Gene lists were generated by searching for "PI3K AND AKT", yielding 605 genes from GeneCards, 116 genes from Reactome, and 359 genes from KEGG. To identify shared genes, we employed an online Venn diagram tool, which revealed 69 overlapping genes across the three databases. These shared genes were subjected to further pathway interaction analysis to explore their functional roles within the PI3K/AKT signaling pathway.

Prognostic analysis and immune cell correlation

In this study, the Kaplan–Meier survival analysis was performed using the Kaplan–Meier Plotter tool (https://kmplot.com/analysis), specifically utilizing the RNA-seq module of the pan-cancer dataset derived from publicly available TCGA databases. Patients with ovarian cancer ($n = 374$) and cervical squamous cell carcinoma ($n = 304$) were selected as the analysis cohorts. The prognostic significance of the identified core genes was evaluated for both ovarian cancer (OV) and cervical squamous cell carcinoma (CESC) using this tool. To evaluate the association between these genes and tumor-infiltrating lymphocytes (TILs), we used the Tumor-Immune System Interaction Database (TISIDB) (http://cis.hku.hk/TISIDB/index.php). The focus was placed on key immune cell types, including activated CD8 + T cells (Act_CD8), activated CD4 + T cells (Act_CD4), NK cells, and B cells. This analysis identified key regulatory genes, such as FLT3, that play a pivotal role in modulating the immune microenvironment and promoting TILs infiltration,

offering potential insights for immune-based therapies. The overall workflow, from gene selection across three major databases to prognostic analysis and immune cell correlation, is illustrated in Supplementary Fig. 2.

Spatial analysis of flt3 and its association with immune cells in ovarian and cervical cancers

Spatial transcriptomics data source and selection

Spatial transcriptomics data were obtained from the 10×Genomics platform (https://www.10xgenomics.com/cn). The ovarian cancer dataset included a serous papillary carcinoma sample (ID: Block 108,906), and the cervical cancer dataset comprised a squamous cell carcinoma sample (ID: Block C00084155.1a). Both datasets were processed using the 10×Genomics Space Ranger pipeline (version 1.3.0), generating standardized gene expression matrices, spatial coordinates, and high-resolution tissue images.

Spatial data preprocessing and integration

Gene expression matrices were imported using the Read10X_h5 function, and high-resolution tissue section images were loaded with the Read10X_Image function. For each sample, we created Seurat objects by integrating spatial coordinates with gene expression data, ensuring accurate alignment between molecular expression profiles and tissue architecture.

Definition of FLT3 high and low expression regions

To analyze the spatial expression patterns of FLT3, we extracted the expression data and defined FLT3-high regions using the 90th percentile as a threshold. Cells with expression levels above this threshold were categorized as FLT3-high, while the rest were considered FLT3-low. This classification provided insight into the distribution of FLT3 across the tumor microenvironment.

Spatial co-expression analysis of FLT3 and immune cell marker genes

We visualized spatial co-expression patterns of FLT3 and immune cell markers using the FeaturePlot function in Seurat. Dual-color plots were generated to highlight regions where FLT3 co-expressed with markers for T cells (CD3D), B cells (CD19), and NK cells (FCGR3A). These plots provided insights into how FLT3 regulates the recruitment and spatial localization of immune cells within the tumor microenvironment, revealing potential immune-modulatory functions of FLT3. The overall workflow for spatial transcriptomics data preprocessing, FLT3 expression region definition, and spatial co-expression analysis is illustrated in Supplementary Fig. 3.

Statistical analysis

All statistical analyses were performed using R with the Seurat, ggplot2, dplyr, and patchwork packages. Differences in immune cell distribution between FLT3-high and FLT3-low regions were evaluated using 2×2 contingency tables, followed by chi-square or Fisher's exact tests. A p-value threshold of < 0.05 was used to determine statistical significance.

Results

Single-cell data preprocessing and quality control

We implemented a rigorous quality control workflow to ensure the reliability of scRNA-seq data. Cells were retained based on the following criteria: (1) expression of at least 200 genes and no more than 9,000 genes; (2) mitochondrial content below 25%. After filtering, 54,079 cells from ovarian cancer (83.4% retention) and 72,007 cells from cervical cancer (95.8% retention) were included in the final analysis (Tables 1 & 2). Key quality metrics, including nFeature (number of detected genes), nCount_RNA (total RNA counts), and percent.mt (mitochondrial content), confirmed the suitability of the retained cells for downstream analysis (Fig. 2).

Table 1 Number of Cells in Each Ovarian Cancer Sample After Filtering

Sample	c1	c2	c3	c4	c5	c6	c7	n1	n2	n3	n4	n5
Cells	**6499**	**3094**	**4304**	**1584**	**5032**	**4108**	**4400**	**6122**	**4962**	**4113**	**6084**	**3777**

* c for cancer samples, n for normal tissue samples

Table 2 Number of Cells in Each Cervical Cancer Sample After Filtering

Sample	c1	c2	c3	c4	c5	n1	n2	n3	n4
Cells	**8786**	**6250**	**2657**	**6788**	**5492**	**10,878**	**8629**	**15,538**	**6989**

* c for cancer samples, n for normal tissue samples

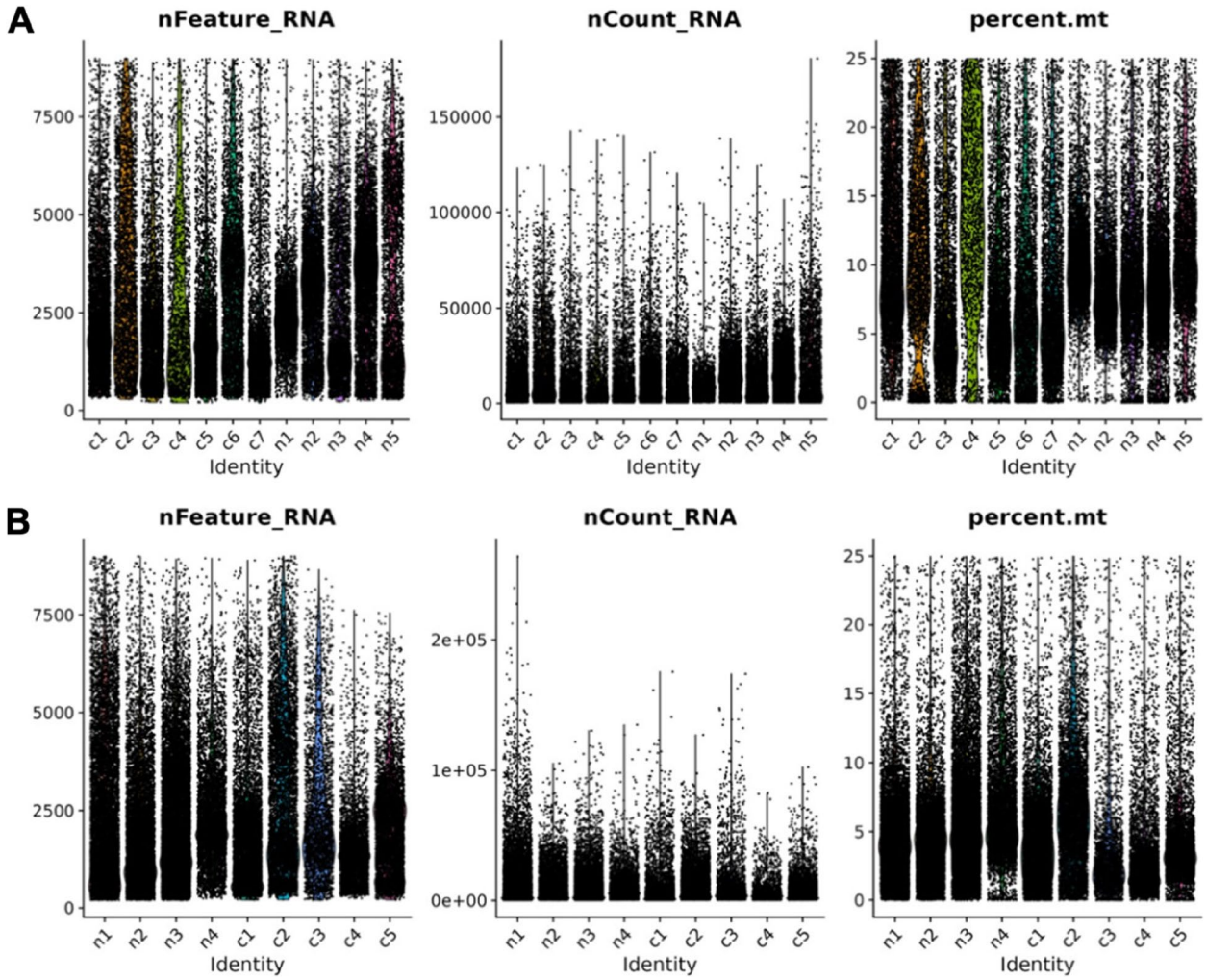

Fig. 2 nFeature_RNA, nCount_RNA, and Proportion of Mitochondrial(percent.mt) Genes After Filtering. **A** Ovarian Cancer; **B** Cervical Cancer

Normalization and Identification of Highly Variable Genes (HVGs)

Following quality control, gene expression values were normalized using the LogNormalize function in Seurat. To capture biologically significant variation, we identified the top 2,000 highly variable genes (HVGs) with the FindVariableFeatures function. Figure 3 illustrates the relationship between average gene expression (x-axis) and standardized variance (y-axis), with red points highlighting the top HVGs.

Batch effect removal using harmony

Given the technical variability across datasets, we employed the Harmony algorithm to remove batch effects while preserving biological variance. As shown in Fig. 4, the Harmony algorithm successfully aligned datasets while retaining meaningful clustering patterns.

Non-Linear dimensionality reduction and cell clustering

To explore high-dimensional scRNA-seq data in a lower-dimensional space, we applied Principal Component Analysis (PCA) followed by non-linear dimensionality reduction using t-distributed Stochastic Neighbor Embedding (t-SNE). Dimensionality reduction was initially performed on the top 2,000 highly variable genes (HVGs) via PCA, and clustering was based on the top 20 principal components (PCs) (Fig. 5A & B).

The t-SNE visualization revealed distinct clusters across both ovarian and cervical cancer datasets, highlighting the transcriptional heterogeneity among different cell populations. In the two-dimensional t-SNE plot,

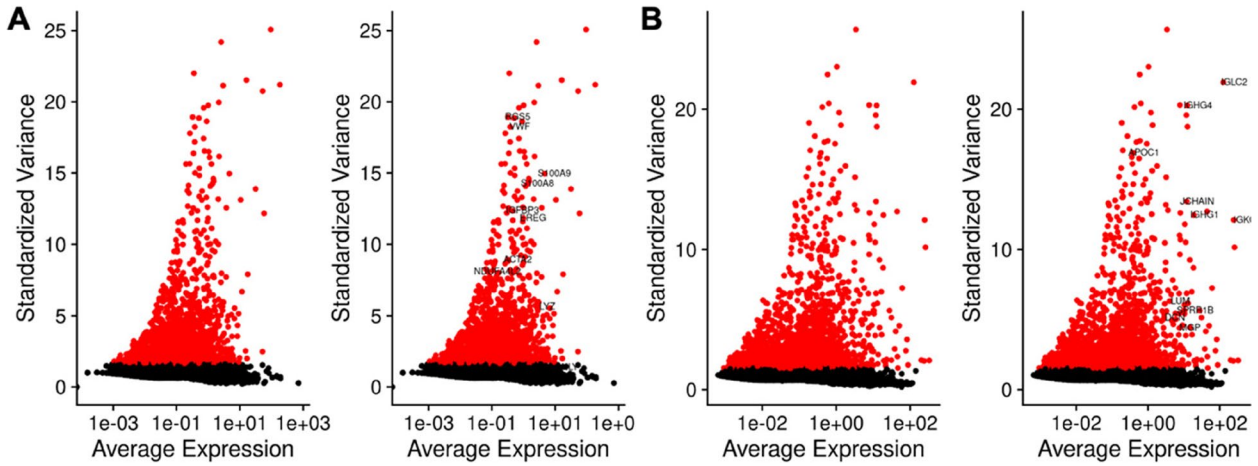

Fig. 3 Identification of HVGs in Cancer. **A** Ovarian Cancer; **B** Cervical Cancer

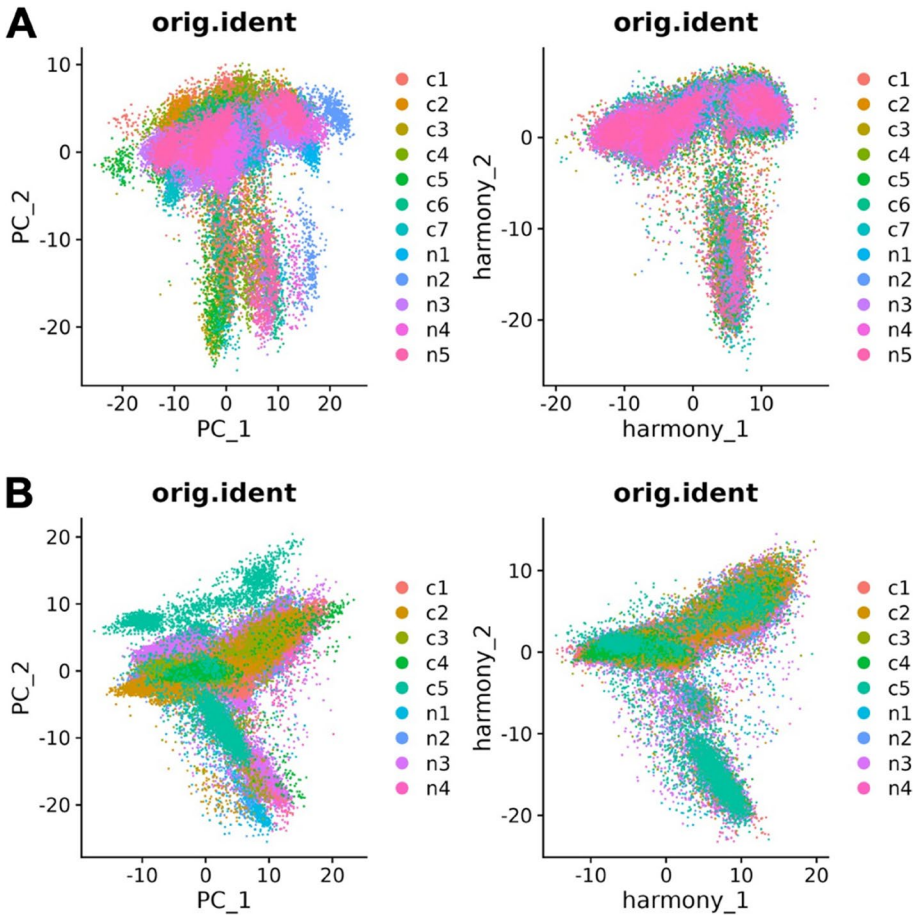

Fig. 4 Comparison Before (Left) and After Harmony (Right). **A** Ovarian Cancer; **B** Cervical Cancer

cells within the same category showed similar transcriptional characteristics, while those from different categories exhibited clear differences. Since t-SNE preserves the local structure of the original high-dimensional space, closely positioned points in the 2D plot typically correspond to cells with similar expression profiles in the

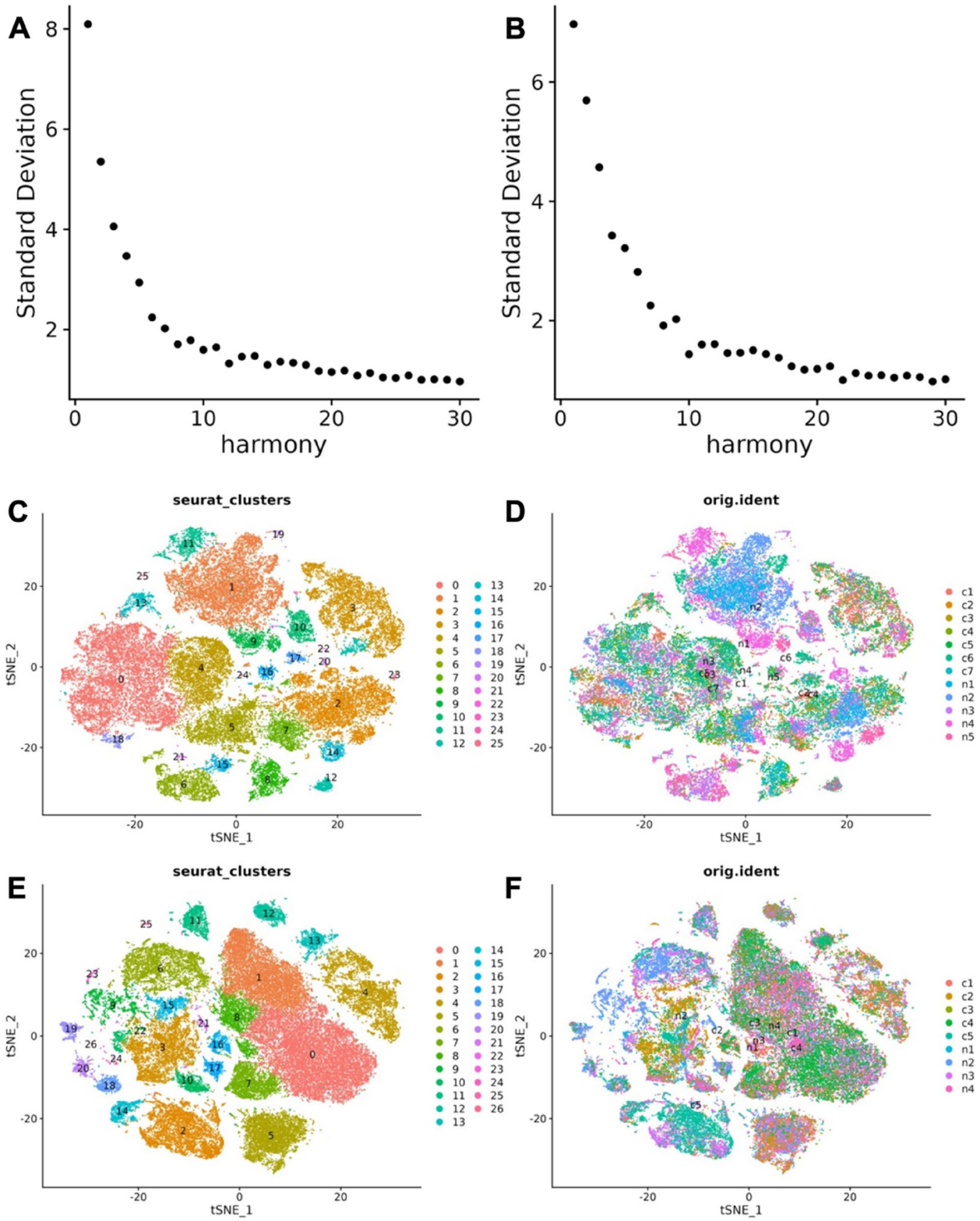

Fig. 5 t-SNE Clustering Plots for Ovarian and Cervical Cancer. **A** Elbow plot for ovarian cancer; **B** Elbow plot for cervical cancer; **C** t-SNE clustering plot for ovarian cancer based on Seurat package clustering results; **D** t-SNE clustering plot for ovarian cancer based on original identity (orig. ident) results; **E** t-SNE clustering plot for cervical cancer based on Seurat package clustering results; **F** t-SNE clustering plot for cervical cancer based on original identity (orig. ident) results

original space. Meanwhile, its non-linear nature ensures that points positioned far apart in the 2D space remain well-separated, minimizing potential overlap between distinct cell types.

Using this approach, 26 clusters were identified in ovarian cancer samples (Fig. 5C & D), and 27 clusters were identified in cervical cancer samples (Fig. 5E & F). Figure 5C and E display the clustering results obtained using the Seurat package, with each point representing a cell, colored according to its assigned cluster. Each cluster reflects a group of cells with similar gene expression profiles. Figure 5D and F present the same t-SNE projection, this time grouping cells based on their original identities (orig. ident). In both cases, the color coding helps visualize the transcriptional characteristics and clustering patterns within the ovarian and cervical cancer datasets, offering valuable insights into biological processes and disease mechanisms.

Immune cell annotation in ovarian and cervical cancer

To define immune cell populations within ovarian and cervical cancers, we annotated each cluster using canonical marker genes. T cells were identified by the expression of CD3D, CD3E, and CD3G; B cells by CD19; and

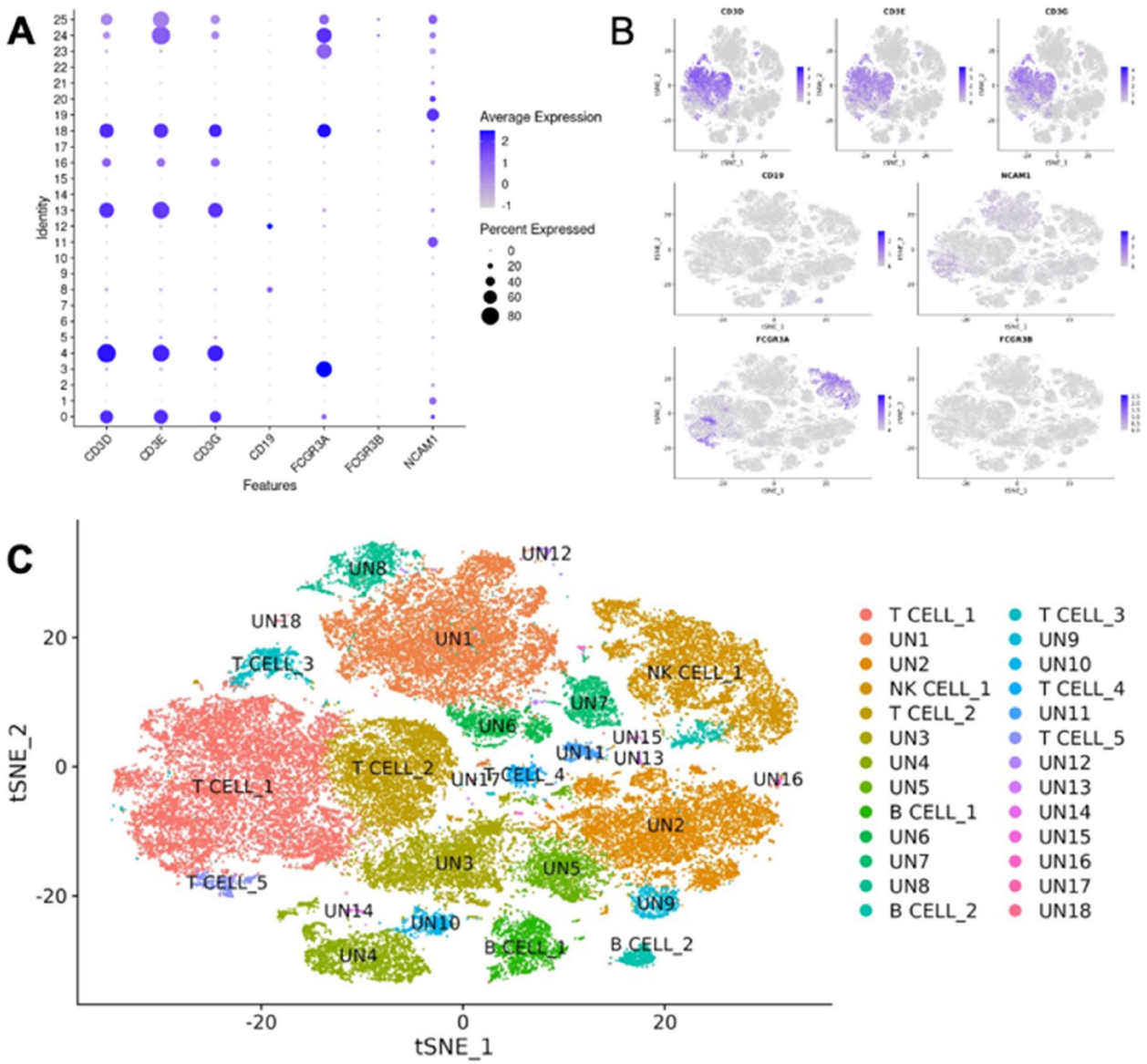

Fig. 6 Annotation of Immune Cells in Ovarian Cancer. **A** DotPlot of specific markers in ovarian cancer; **B** Expression distribution of specific markers in t-SNE for ovarian cancer; **C** t-SNE distribution of ovarian cancer after cell annotation

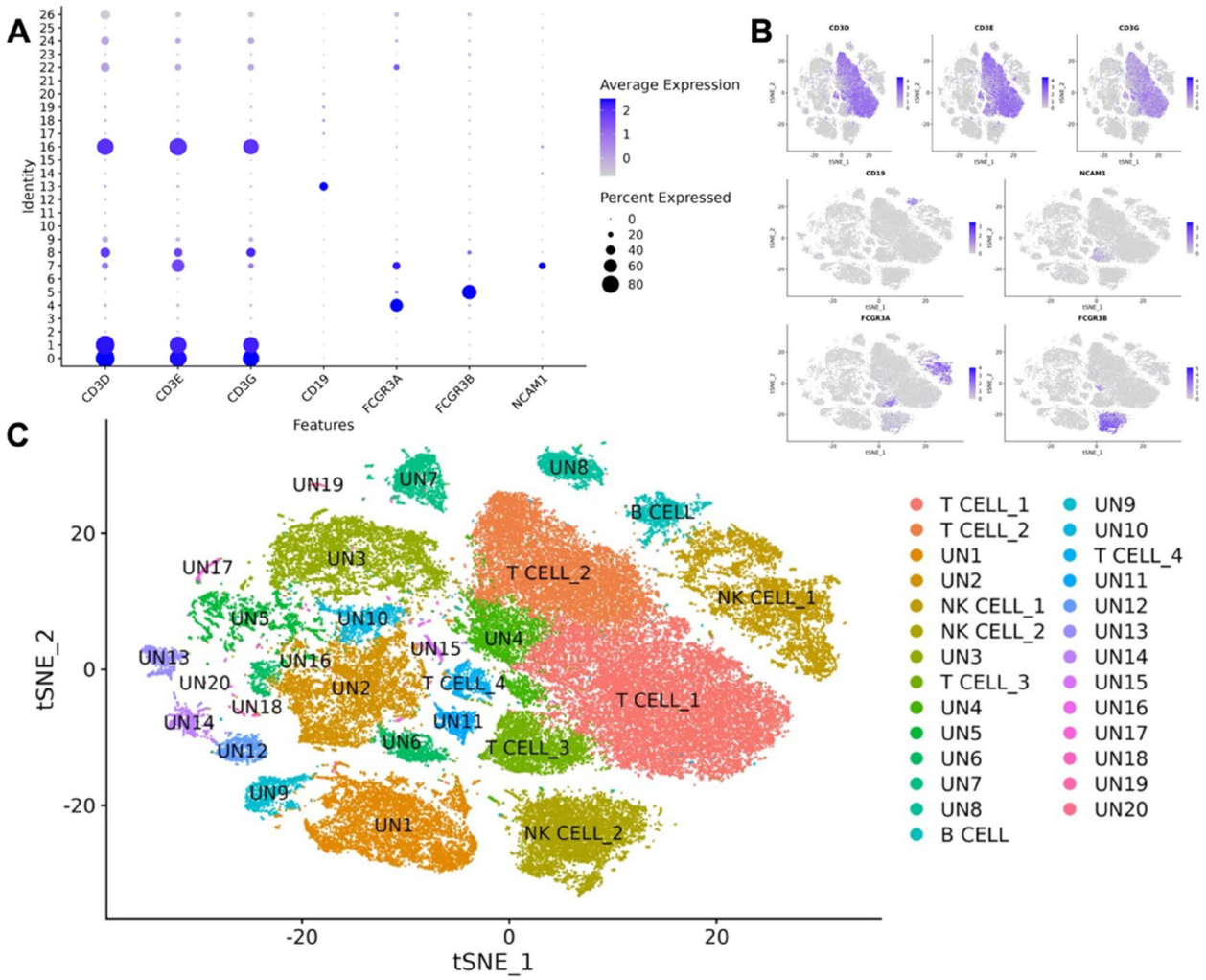

Fig. 7 Annotation of Immune Cells in Cervical Cancer. **A** DotPlot of specific markers in cervical cancer; **B** Expression distribution of specific markers in t-SNE for cervical cancer; **C** t-SNE distribution of cervical cancer after cell annotation

NK cells by FCGR3A, FCGR3B, and NCAM1. The annotation results are shown in Fig. 6A for ovarian cancer and Fig. 7 for cervical cancer. Each dot represents a cluster, with dot size indicating the proportion of cells expressing a given marker and color intensity reflecting the average expression level. This comprehensive annotation enabled us to accurately classify each cluster into distinct immune cell subtypes. Based on these criteria, ovarian cancer clusters 0, 4, 13, 16, and 18 were annotated as T cells, clusters 8 and 12 as B cells, and cluster 3 as NK cells (Fig. 6). Similarly, cervical cancer clusters 0, 1, 7, and 16 were classified as T cells, cluster 13 as B cells, and clusters 4 and 5 as NK cells. This annotation provided a robust framework for downstream differential gene expression.

Screening and pathway analysis of common differential genes in ovarian and cervical cancer

T cells are the largest population of tumor-infiltrating lymphocytes (TILs) and play a central role in anti-tumor immunity, making them an ideal initial focus for analysis. Prioritizing T cells allowed us to efficiently identify biologically significant differentially expressed genes and establish a foundation for broader investigations.

Using the FindMarkers function, we identified differentially expressed genes (DEGs) between tumor and normal tissues for T cells in ovarian and cervical cancer. By applying an adjusted *P*-value threshold of < 0.05, we identified 4,362 DEGs in ovarian cancer and 3,360 DEGs in cervical cancer, with 2,143 shared genes between the two cancer types (Fig. 8A).

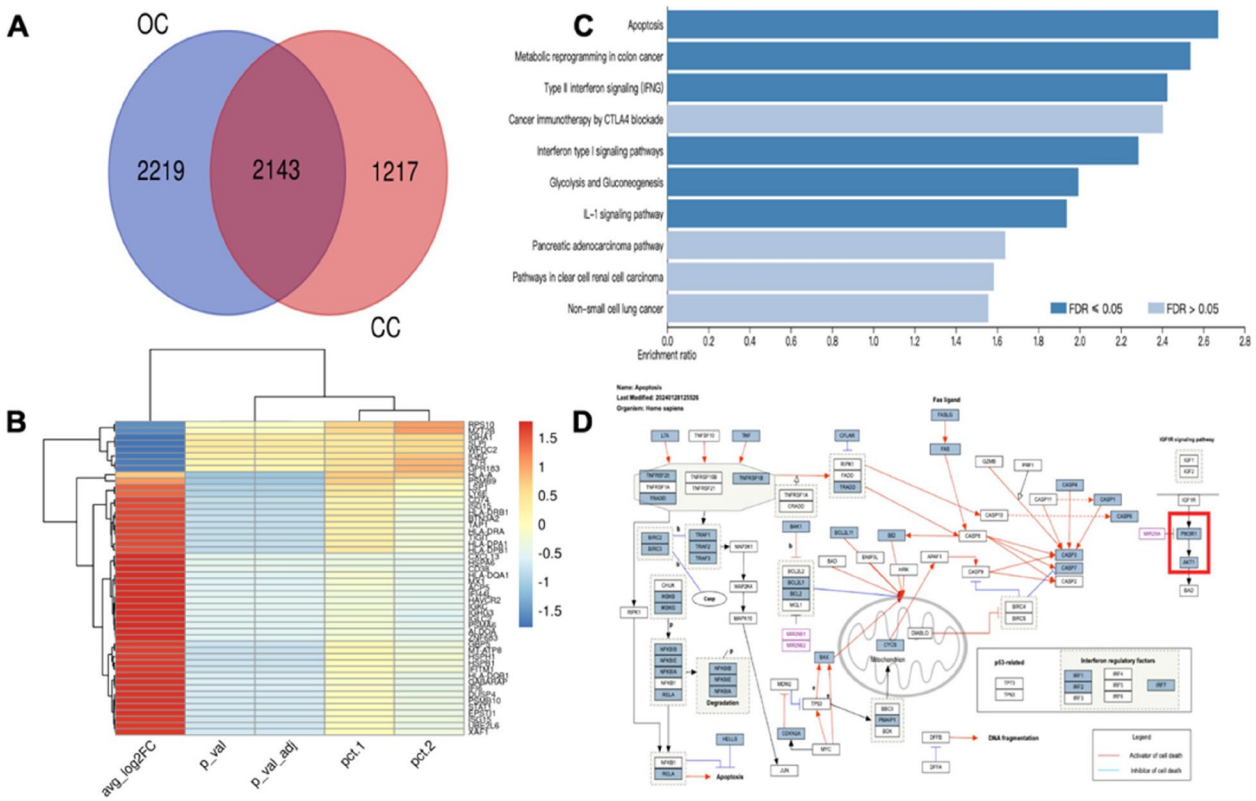

Fig. 8 Screening and Pathway Analysis of Common Differential Genes in Ovarian and Cervical Cancer. **A** Venn diagram showing shared differential genes between ovarian and cervical cancer. **B** Heatmap of the top 50 shared differential genes, with expression changes quantified by avg_log2FC (red: upregulation, blue: downregulation). Statistical significance is shown by *P*_val and *P*_val_adj (darker colors indicate higher significance). *"pct1" and "pct2" represent the proportion of cells expressing a gene in the normal and tumor groups, respectively. **C** WikiPathways cancer enrichment analysis for shared differential genes. **D** Detailed apoptosis pathway from WikiPathways, highlighting key signaling components and interactions

Figure 8B presents a clustered heatmap of the top 50 shared genes commonly expressed in ovarian and cervical cancers. The extent of gene expression changes is quantified by the average log2 fold change (avg_log2FC), with red indicating significant upregulation and blue indicating significant downregulation. Statistical significance is represented by the *p*-value (P_val) and adjusted *p*-value (P_val_adj), with darker colors reflecting higher levels of significance. It is important to note that color intensity does not directly correspond to the numerical values of the p-values. In differential expression analysis, the *p*-value is calculated through statistical testing and reflects the significance of the difference in gene expression between two groups. Fold change, by contrast, measures the magnitude of these expression differences. Small *p*-values are typically associated with large fold changes, indicating pronounced differences between groups. Conversely, smaller fold changes are often linked to reduced statistical significance and consequently larger p-values. The top 50 shared DEGs are visualized in a heatmap (Fig. 8B), highlighting the distinct transcriptional signatures of T cells in ovarian and cervical cancers.

To investigate the possible pathways associated with the shared DEGs, we utilized the WebGestalt platform to perform WikiPathways cancer pathway enrichment analysis. WikiPathways cancer provides a pathway collection specifically tailored for cancer research, making it the most suitable choice for this study. As shown in Fig. 8C, apoptosis emerged as the most significantly enriched pathway for the shared DEGs in ovarian and cervical cancers. Building on the enrichment analysis, we further examined the detailed apoptosis pathway (also called WP254 in WebGestalt) to explore the specific genes and molecular networks involved. The pathway diagram in Fig. 8D illustrates the intricate signaling components and interactions within the apoptosis pathway. Our analysis revealed that the IGF1R signaling pathway, a subset of the PI3K/AKT pathway, plays a pivotal role in regulating apoptosis. The pathway diagram in Fig. 8D specifically underscores the significance of PI3K/AKT signaling in modulating downstream apoptotic processes, providing a compelling rationale for further investigation of this signaling cascade. Additionally, our previously published work strongly supports that dual

knockout of AKT1/2 significantly reduced early apoptosis in CD8 + TILs [28], reinforcing the scientific validity and importance of focusing on the PI3K/AKT pathway as a key target. This rationale underpins our decision to prioritize the PI3K/AKT signaling pathway for the next phase of our research.

Identifying PI3K/AKT signaling pathway related genes from three bioinformatics websites

In this study, we firstly identified 69 PI3K/AKT-related common genes using GeneCards, Reactome, and KEGG databases (Table 3& Fig. 9A), and refined the list to 45 core genes using the MCODE plugin in Cytoscape (Table 4& Fig. 9B). By inputting the aforementioned 45 core genes into the Kaplan–Meier Plotter database, we screened for genes that are statistically significant for prognosis in both cervical and ovarian cancer. A total of 9 genes met these criteria: AKT1, EGF, EGFR, ERBB2, FGF5, FGFR4, FLT3, IRS1, and PIK3R2. (Fig. 9C).

Correlation between prognostic gene expression and tumor-infiltrating lymphocytes in ovarian and cervical cancers

To investigate the relationship between key prognostic genes and tumor-infiltrating lymphocytes (TILs) in ovarian and cervical cancers, we utilized the Tumor-Immune System Interaction Database (TISIDB). Specifically, we analyzed the correlation of nine core genes (AKT1, EGF, EGFR, ERBB2, FGF5, FGFR4, FLT3, IRS1, and PIK3R2) with the abundance of activated CD8 T cells (Act_CD8) and activated CD4 T cells (Act_CD4) in both ovarian cancer (OV) and cervical squamous cell carcinoma (CESC). Using Spearman correlation and statistical significance tests, we observed that high expression levels of ERBB2, IRS1, and PIK3R2 were significantly negatively correlated with the abundance of both Act_CD8 and Act_CD4 cells, suggesting a potential role in immune suppression (Fig. 10A, C&D). In contrast, FLT3 expression showed a significant positive correlation with these immune cells, indicating its potential role in enhancing immune activation (Fig. 10B). To further understand the broader impact of these genes on the tumor immune microenvironment, we extended our analysis to other immune cell types, such as natural killer (NK) cells and B cells.

The results revealed that high FLT3 expression was positively correlated with NK cell abundance in both OV and CESC, suggesting an immune-stimulatory effect. Conversely, PIK3R2 exhibited a significant negative correlation with NK cells, indicating an immune-suppressive role, while ERBB2 and IRS1 showed no significant correlation (Fig. 11). Our next step is to further investigate the relationship between the FLT3 and PIK3R2 genes and B cells. Similar trends were observed for B cells, where FLT3 was positively associated with increased B cell infiltration, whereas PIK3R2 was negatively correlated with B cell abundance in OV but not in CESC (Fig. 12). Collectively, these findings suggest that FLT3 may play a crucial role in promoting immune activation across various immune cell types in both cancers.

In summary, FLT3 expression in cervical squamous cell carcinoma (CESC) and ovarian serous cystadenocarcinoma (OV) is significantly associated with increased infiltration of activated immune cells, including CD4 and CD8 T cells, NK cells, and B cells, suggesting its potential as a target for enhancing anti-tumor immunity in these cancers.

Spatial co-expression analysis of FLT3 and immune cells

To determine the spatial distribution of FLT3 and its association with immune cells, we performed spatial co-expression analysis in ovarian and cervical cancer samples. FLT3 expression levels were stratified using the 90th percentile as a threshold, categorizing cells into FLT3-high and FLT3-low regions to delineate spatial patterns and assess immune cell localization in the tumor microenvironment. Figure 13A and B show the spatial co-expression of FLT3 with T cell, B cell, and NK cell markers in both cancers. Regions of co-expression, marked by red dashed circles, suggest that FLT3 is spatially associated with increased infiltration of these immune cells.

Quantitative analysis further demonstrated that in ovarian cancer, FLT3-high regions were significantly enriched for B cells ($P = 0.0001$), while no significant differences were observed for T cells ($P = 0.067$) or NK cells ($P = 0.66$). In contrast, in cervical cancer, all three immune cell types showed significantly higher

Table 3 Common Genes Related to the PI3K/AKT Signaling Pathway from Three Databases

Number	Genes Name
69	AKT1 AKT2 AKT3 AREG BAD CASP9 CD19 CDKN1A CDKN1B CHUK CREB1 EGF EGFR ERBB2 ERBB3 ERBB4 EREG FGF1 FGF10 FGF16 FGF17 FGF18 FGF19 FGF2 FGF20 FGF22 FGF23 FGF3 FGF4 FGF5 FGF6 FGF7 FGF8 FGF9 FGFR1 FGFR2 FGFR3 FGFR4 FLT3 FLT3LG FOXO3 GRB2 GSK3B HGF IRS1 KIT KITLG MDM2 MET MLST8 MTOR NR4A1 PDGFA PDGFB PDGFRA PDGFRB PDPK1 PIK3AP1 PIK3CA PIK3CB PIK3CD PIK3R1 PIK3R2 PIK3R3 PTEN RAC1 RPS6KB2 TGFA TSC2

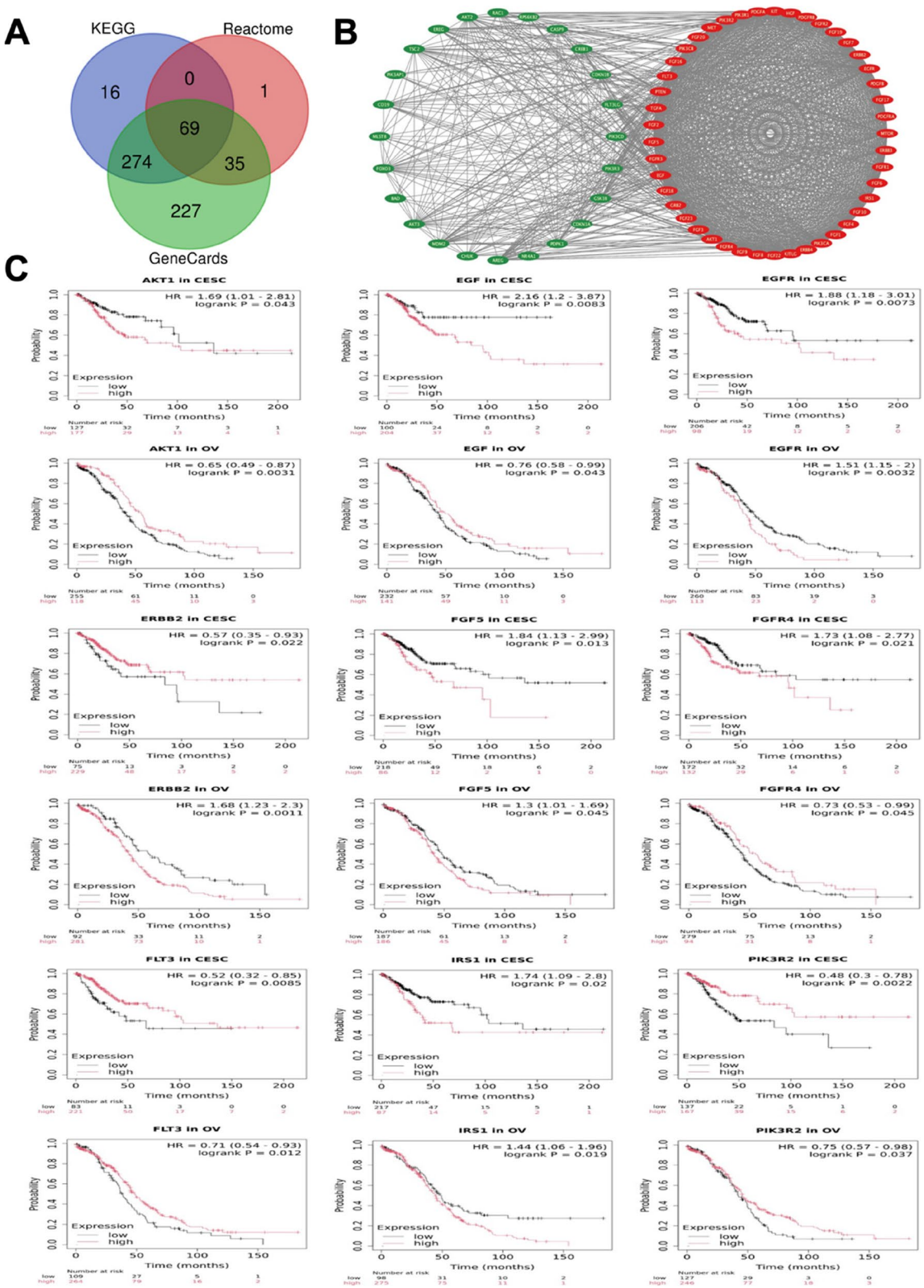

Fig.9 Genes of the PI3K/AKT Signaling Pathway Related to Prognosis in Ovarian and Cervical Cancer. **A** Venn diagram of common genes in the PI3K/AKT signaling pathway; **B** Visualization of core genes in the PI3K/AKT signaling pathway; **C** Common genes related to prognosis in ovarian and cervical cancer

Table 4 Core Genes of the PI3K/AKT Signaling Pathway

Number	Genes Name
45	AKT1 EGF EGFR ERBB2 ERBB3 ERBB4 FGF1 FGF2 FGF3 FGF4 FGF5 FGF6 FGF7 FGF8 FGF9 FGF10 FGF16 FGF17 FGF18 FGF19 FGF20 FGF22 FGF23 FGFR1 FGFR2 FGFR3 FGFR4 FLT3 GRB2 HGF IRS1 KIT KITLG MET MTOR PDGFA PDGFB PDGFRA PDGFRB PIK3CA PIK3CB PIK3R1 PIK3R2 PTEN TGFA

proportions in FLT3-high regions (T cells: $P=0.0001$; B cells: $P=0.008$; NK cells: $P=0.046$) (Table 5& Fig.C&D). These results suggest that high FLT3 expression may be associated with enhanced infiltration of tumor-infiltrating lymphocytes (TILs), influencing their spatial distribution and function within the tumor microenvironment.

Discussion

Based on our clinical observations and previous studies, TILs have been shown to significantly improve survival outcomes in ovarian and cervical cancers, suggesting the presence of shared regulatory mechanisms. However, the molecular underpinnings of these mechanisms remain poorly understood. To address this gap, our study takes an innovative approach by integrating single-cell RNA sequencing (scRNA-seq) data with spatial transcriptomics—a combination rarely applied in these malignancies. This dual-layered analysis allowed us to uncover shared differentially expressed genes (DEGs) and reveal how these genes operate in both molecular and spatial dimensions, offering novel insights into immune regulation in ovarian and cervical cancers. Using scRNA-seq data from the GEO database, we employed Seurat and Harmony for data processing and batch effect correction, followed by dimensionality reduction with t-SNE and immune cell annotation based on canonical markers. This analysis identified PI3K/AKT signaling as a pivotal pathway regulating immune cells in both cancers, providing a unified explanation for their shared immune-regulatory mechanisms. A particularly innovative aspect of this study is the integration of spatial transcriptomics, which enabled us to map FLT3 expression within the tumor microenvironment and its spatial co-localization with immune cells. Our results demonstrate that FLT3-high regions are enriched with T cells, NK cells, and B cells, especially in cervical cancer. This spatial insight emphasizes the role of FLT3 not only as a molecular regulator but also as a key player in the spatial orchestration of immune responses within the tumor microenvironment. Such insights are critical for understanding the spatial dynamics of tumor-infiltrating lymphocytes (TILs) and their potential therapeutic modulation.

FLT3, previously studied primarily in acute myeloid leukemia (AML), has recently been implicated in solid tumors such as NSCLC, where it has been linked to enhanced immune cell infiltration and improved prognosis [29]. Our findings expand the role of FLT3 to ovarian and cervical cancers, demonstrating that it functions as an immune modulator through the PI3K/AKT pathway, enhancing TILs recruitment and activity. This is the first study to provide spatially resolved evidence of FLT3's role in promoting immune responses in these cancers, underscoring its potential as a novel immunotherapeutic target.

Our results align with previous studies showing that FLT3 promotes cell proliferation, inhibits apoptosis, and regulates differentiation through multiple signaling pathways, including RAS/MAPK, JAK/STAT, and PI3K/AKT [30]. Among these, the PI3K/AKT pathway plays a critical role in the development and function of immune cells and is essential for maintaining immune homeostasis [31, 32]. However, aberrant activation of this pathway has been associated with poor prognosis in various cancers, highlighting its dual role in tumor biology and immune regulation [33–36]. In our study, WikiPathways cancer pathway pathway enrichment analyses of shared DEGs identified the PI3K/AKT pathway as a key regulator of apoptosis. This finding is consistent with our previous research, where we demonstrated that knocking out AKT1/2 reduces early apoptosis in CD8 + TILs, thereby enhancing their stemness and anti-tumor activity [28]. Our current results suggest that high FLT3 expression may enhance the stemness and function of TILs through the PI3K/AKT pathway, contributing to improved immune responses and prolonged patient survival in ovarian and cervical cancers.

In ovarian cancer, the TME is typically more immunosuppressive. Studies have shown elevated levels of immune checkpoint molecules such as PD-1 and CTLA-4 [37], as well as immunosuppressive factors like TGF-β and IL-10 [38], within ovarian cancer tissues. These elements hinder T-cell activation and infiltration. Additionally, the accumulation of tumor-associated macrophages (TAMs) and regulatory T cells (Tregs) further dampens the anti-tumor immune response [39]. Consequently, even if FLT3 is highly expressed and potentially promotes immune cell infiltration, the overall immunosuppressive environment may still impede effective

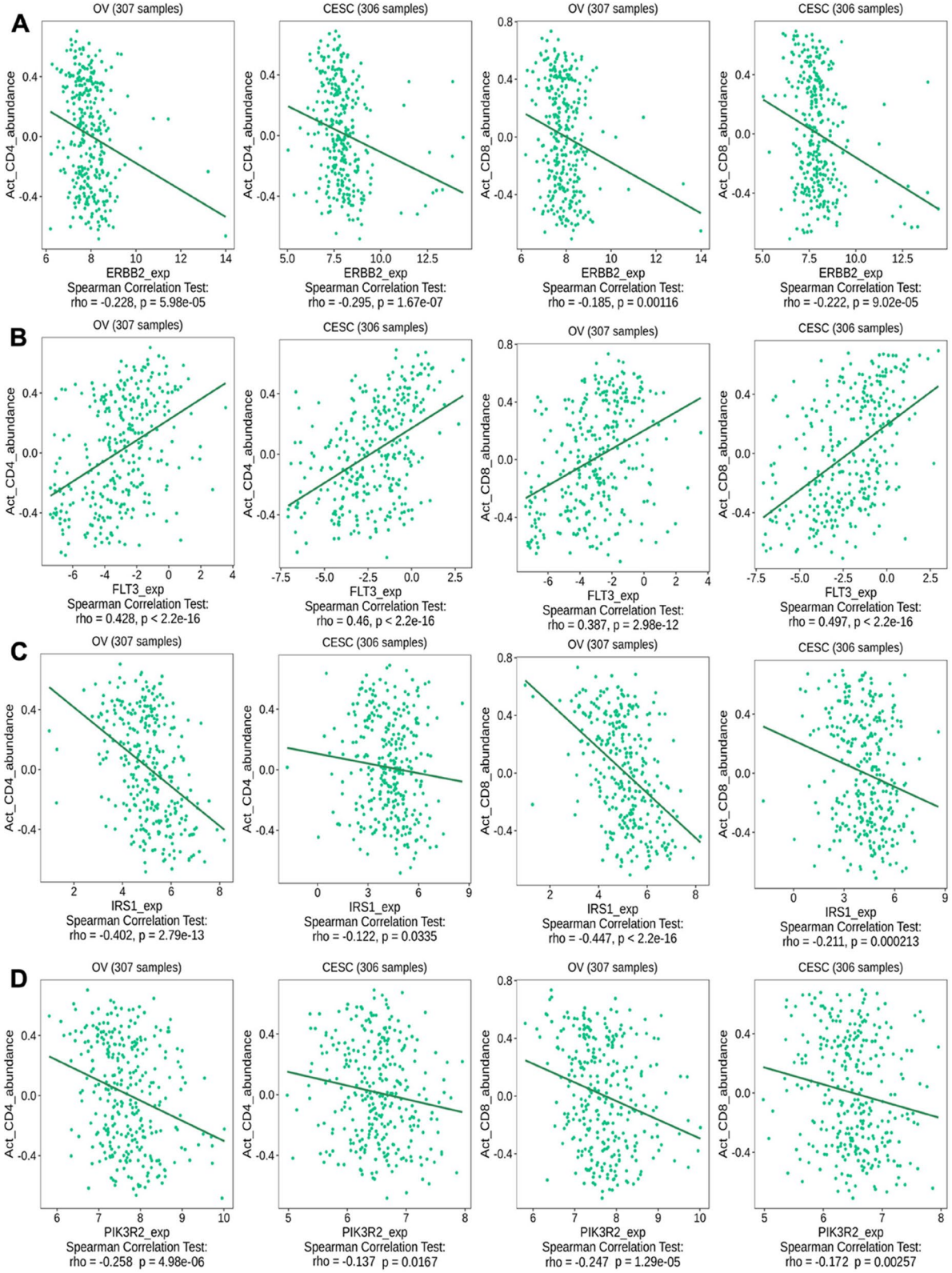

Fig.10 Scatter Plot Analysis of Gene Expression and Correlation with CD4 T & CD8 T Cells. **A** ERBB2_exp; **B** FLT3_exp; **C** IRS1_exp; **D** PIK3R2_exp

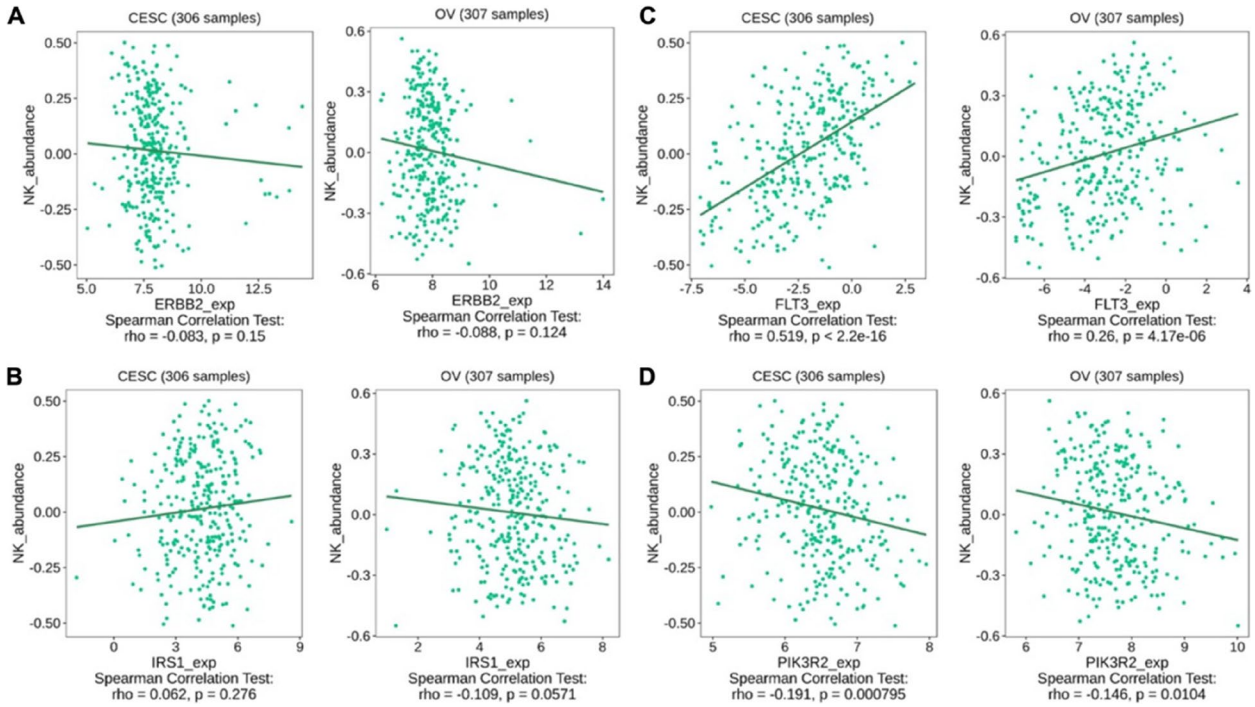

Fig.11 Scatter Plot Analysis of Gene Expression and Correlation with NK Cells. **A** ERBB2_exp; **B** IRS1_exp; **C** FLT3_exp; **D** PIK3R2_exp

T-cell accumulation and function, leading to suboptimal outcomes with immunotherapy. In contrast, the TME of cervical cancer exhibits more immune-activating characteristics, primarily due to the persistent immune response triggered by high-risk human papillomavirus (HPV) infection. HPV not only activates the host immune system but also enhances immune surveillance mechanisms, facilitating the infiltration of immune cells, particularly CD8 + T cells [40, 41]. This immune-activated state renders cervical cancer patients more responsive to immunotherapy [42]. Moreover, ovarian cancer may employ various immune evasion strategies to suppress immune cell infiltration and function. For instance, research indicates that ovarian cancer can evade immune detection through multiple mechanisms, resulting in significant differences among different subtypes and even between different tumor sites within the same patient [43]. These complex immune evasion tactics further diminish the efficacy of immunotherapy [44]. In summary, the significant differences between ovarian and cervical cancers in terms of tumor microenvironment (TME), immune cell infiltration characteristics, and immune evasion mechanisms may explain their disparate responses to immunotherapy. These conclusions align with our study's findings that high FLT3 expression correlates with increased infiltration of CD4 and CD8 T cells, B cells, and NK cells, particularly in cervical cancer, further demonstrating the accuracy and rigor of this research.

Currently, research on FLT3-targeted therapies has predominantly focused on the development of FLT3 inhibitors, especially in the context of acute myeloid leukemia (AML). FLT3 inhibitors such as Midostaurin [45] and Gilteritinib [46] have shown significant progress in clinical applications. These drugs exert their effects by inhibiting the activation of the FLT3 signaling pathway, thereby suppressing tumor cell proliferation and inducing apoptosis. Meanwhile, FLT3 agonists represent another promising avenue. FLT3 agonists, through the activation of FLT3 receptors, have the potential to enhance immune cell function, particularly T cells, thereby improving the immune system's ability to recognize and eliminate tumors. For instance, studies have demonstrated that the FLT3 agonist Fc-fusion protein (GS-3583) exhibits the capacity to expand circulating dendritic cells (cDCs) in healthy volunteers [47] and patients with advanced solid tumors [48], which could subsequently enhance T-cell-mediated antitumor activity. Combination therapies also constitute an important strategy. In murine models, the combined use of FLT3 ligand (Flt3L) and PD-1 antibody fusion protein (PD-1Ab7, a fusion of CCL7 and an scFv of anti-PD-1) significantly promoted the generation and proliferation of cDC1s, while enhancing T-cell activation and expansion within the tumor microenvironment. This synergistic effect led to markedly improved antitumor immune responses [49]. Moreover, the combination of FLT3 inhibitors with chemotherapy or other targeted

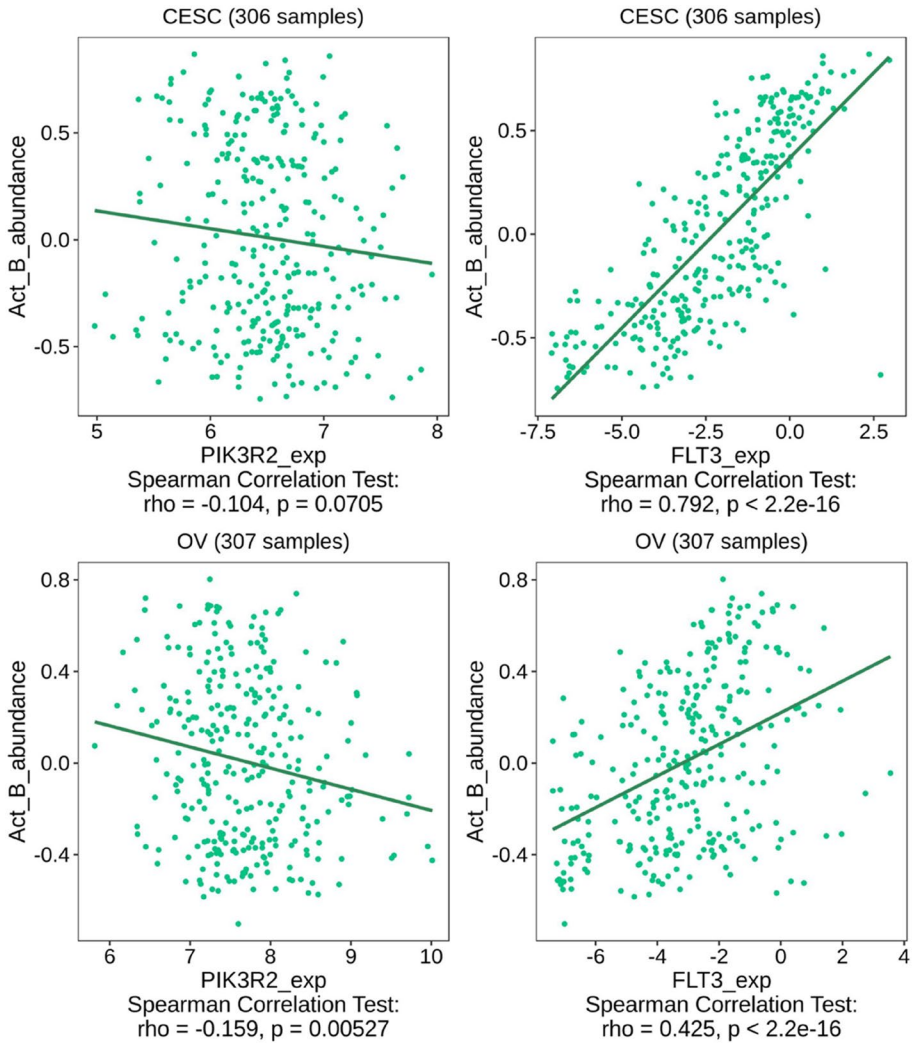

Fig.12 Scatter Plot Analysis of Gene FLT3 and PIK3R2 Expression and Correlation with B Cells

therapies offers potential for overcoming drug resistance and improving patient outcomes, making it a promising therapeutic strategy [50]. However, clinical studies on FLT3-targeted therapies for ovarian and cervical cancers remain relatively limited. Future investigations could explore the application of FLT3 inhibitors in these malignancies and evaluate their combination with existing treatment modalities such as chemotherapy, immunotherapy, or other targeted therapies.

Despite providing new insights, our study has certain limitations. Variability in cell isolation, sequencing depth, and the use of publicly available GEO datasets may impact the reproducibility and generalizability of our findings. Future studies with larger, more diverse cohorts will be needed for validation. While spatial transcriptomics adds spatial context, it may introduce sampling bias and be influenced by tissue heterogeneity, particularly in complex tumor microenvironments. Differences in immune cell distribution, vascular patterns, and tumor composition across regions can affect gene expression analyses. Finally, as our conclusions are primarily based on bioinformatics analyses, experimental validation through in vivo and in vitro studies will be essential to confirm the mechanistic role of FLT3 and assess its therapeutic potential, particularly for patients resistant to conventional therapies.

Conclusion

In summary, our study reveals that FLT3 enhances TIL function through the PI3K/AKT pathway, offering a novel immunotherapeutic target for ovarian and cervical cancers. Beyond its established role in hematologic malignancies, FLT3 shows potential in solid tumors by promoting immune cell infiltration

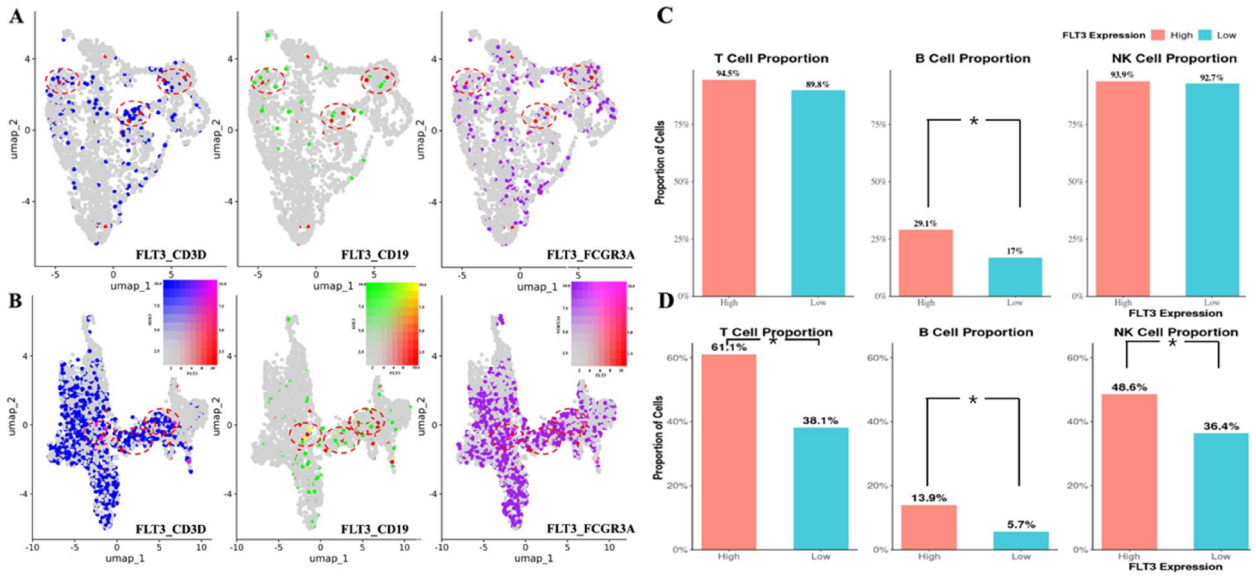

Fig. 13 Spatial Co-expression Analysis of FLT3 and Immune Cells of Ovarian and Cervical Cancers. The red circles represent regions of spatial co-expression between FLT3 and immune cells. **A**&**D** Cervical Cancer; **B**&**C** Ovarian Cancer. *$p < 0.05$

Table 5 Proportions of T Cells, B Cells, and NK Cells in FLT3-High and FLT3-Low Regions in Ovarian and Cervical Cancers

FLT3_Expression	Ovarian Cancer			Cervical Cancer		
	T_Cells	B_Cells	NK_Cells	T_Cells	B_Cells	NK_Cells
High	0.945	0.291	0.939	0.611	0.139	0.486
Low	0.898	0.17	0.927	0.381	0.0565	0.364
***P*_Value**	0.067	**0.0001**	0.66	**0.0001**	**0.008**	**0.046**

and activation, improving patient prognosis. Using a reverse-engineering approach, we identified FLT3 as a key regulator of anti-tumor immunity, with promising therapeutic implications, particularly for patients resistant to conventional treatments. Future clinical trials will be essential to validate the efficacy of FLT3-targeted strategies, paving the way for new treatment options in cancer immunotherapy.

Supplementary Information

The online version contains supplementary material available at https://doi.org/10.1186/s13048-025-01592-8.

Supplementary Material 1.

Supplementary Material 2.

Supplementary Material 3.

Acknowledgements
The authors would like to thank the GEO database and 10x Genomics platform for providing the single-cell RNA sequencing and spatial transcriptomics data that made this research possible. We also extend our gratitude to the anonymous reviewers for their insightful comments and suggestions, which have significantly improved the quality of this manuscript.

Authors' contributions
Feng Hao and Zhang Yan were responsible for data curation, formal analysis, methodology design, and writing the original draft. Luo Shen assisted with data curation, analysis, and visualization. Wang Hui and Qiu Ling assisted with methodology design, validation, and the review and editing of the manuscript. Yang Xiaoyu and Jiang Hua were responsible for supervision, project management, and the conceptualization of the study.

Data availability
The datasets generated and analyzed in this study are available in the Gene Expression Omnibus (GEO) database under the following accession numbers: GSE184880, GSE197461, and GSE208653. The spatial transcriptomics data were obtained from the 10×Genomics platform, including the ovarian cancer dataset (Serous papillary carcinoma, ID: Block 108,906) and the cervical cancer dataset (Squamous cell carcinoma, ID: Block C00084155.1a). All datasets are publicly accessible through their respective repositories. Any additional data or materials supporting the conclusions of this article are available from the corresponding author upon reasonable request.

Declarations

Competing interests
The authors declare no competing interests.

Received: 17 September 2024 Accepted: 6 January 2025
Published online: 25 January 2025

References

1. Fadl J, Aljuhani RA, Albog YH, Khraisat AF, Alsubaie KA. Role of microRNA in sex steroid hormones signaling and its effect in regulation of endometrial, ovarian, and cervical cancer: a literature review. Cureus. 2024;16:e54773.
2. Bejarano L, Jordão MJ, Joyce JA. Therapeutic targeting of the tumor microenvironment. Cancer Discov. 2021;11:933–59.
3. El-Tanani M, Rabbani SA, Babiker R, Rangraze I, Kapre S, Palakurthi SS, Alnuqaydan AM, Aljabali AA, Rizzo M, El-Tanani Y. Unraveling the tumor microenvironment: insights into cancer metastasis and therapeutic strategies. Cancer Letters. 2024;591:216894.
4. Naser R, Fakhoury I, El-Fouani A, Abi-Habib R, El-Sibai M. Role of the tumor microenvironment in cancer hallmarks and targeted therapy. Int J Oncol. 2022;62:23.
5. Amer HT, Stein U, El Tayebi HM. The Monocyte, a Maestro in the Tumor Microenvironment (TME) of Breast Cancer. Cancers (Basel). 2022;14(21):5460.
6. Lu C, Liu Y, Ali NM, Zhang B, Cui X. The role of innate immune cells in the tumor microenvironment and research progress in anti-tumor therapy. Front Immunol. 2022;13:1039260.
7. de Visser KE, Joyce JA. The evolving tumor microenvironment: From cancer initiation to metastatic outgrowth. Cancer Cell. 2023;41:374–403.
8. Liu Y, Zhang Q, Xing B, Luo N, Gao R, Yu K, Hu X, Bu Z, Peng J, Ren X. Immune phenotypic linkage between colorectal cancer and liver metastasis. Cancer Cell. 2022;40:424-437 e425.
9. Globus O, Sagie S, Lavine N, Barchana DI, Urban D. Early mortality in metastatic cancer: A SEER population data analysis. J Clin Oncol. 2021;39:15_suppl.e18789.
10. Ciarka A, Piatek M, Peksa R, Kunc M, Senkus E. Tumor-Infiltrating Lymphocytes (TILs) in Breast Cancer: Prognostic and Predictive Significance across Molecular Subtypes. Biomedicines. 2024;12(4):763.
11. Hong JJ, Rosenberg SA, Dudley ME, Yang JC, White DE, Butman JA, Sherry RM. Successful treatment of melanoma brain metastases with adoptive cell therapy. Clin Cancer Res. 2010;16:4892–8.
12. Chen T, Cao Z, Sun Y, Huang J, Shen S, Jin Y, Jiang L, Wen F, Zhao X, Zhang D, et al. Neoadjuvant chemoimmunotherapy increases tumor immune lymphocytes infiltration in resectable non-small cell lung cancer. Ann Surg Oncol. 2023;30:7549–60.
13. Poch M, Hall M, Joerger A, Kodumudi K, Beatty M, Innamarato PP, Bunch BL, Fishman MN, Zhang J, Sexton WJ, et al. Expansion of tumor infiltrating lymphocytes (TIL) from bladder cancer. Oncoimmunology. 2018;7:e1476816.
14. Braun MW, Abdelhakim H, Li M, Hyter S, Pessetto Z, Koestler DC, Pathak HB, Dunavin N, Godwin AK. Adherent cell depletion promotes the expansion of renal cell carcinoma infiltrating T cells with optimal characteristics for adoptive transfer. J Immunother Cancer. 2020;8(2):e000706.
15. Aydin AM, Hall M, Bunch BL, Branthoover H, Sannasardo Z, Mackay A, Beatty M, Sarnaik AA, Mullinax JE, Spiess PE, Pilon-Thomas S. Expansion of tumor-infiltrating lymphocytes (TIL) from penile cancer patients. Int Immunopharmacol. 2021;94:107481.
16. Ko A, Coward VS, Gokgoz N, Dickson BC, Tsoi K, Wunder JS, Andrulis IL. Investigating the Potential of Isolating and Expanding Tumour-Infiltrating Lymphocytes from Adult Sarcoma. Cancers (Basel). 2022;14(3):548.
17. Liu Z, Meng Q, Bartek J Jr, Poiret T, Persson O, Rane L, Rangelova E, Illies C, Peredo IH, Luo X, et al. Tumor-infiltrating lymphocytes (TILs) from patients with glioma. Oncoimmunology. 2017;6:e1252894.
18. Meng Q, Liu Z, Rangelova E, Poiret T, Ambati A, Rane L, Xie S, Verbeke C, Dodoo E, Del Chiaro M, et al. Expansion of tumor-reactive T cells from patients with pancreatic cancer. J Immunother. 2016;39:81–9.
19. Pedersen M, Westergaard MCW, Milne K, Nielsen M, Borch TH, Poulsen LG, Hendel HW, Kennedy M, Briggs G, Ledoux S, et al. Adoptive cell therapy with tumor-infiltrating lymphocytes in patients with metastatic ovarian cancer: a pilot study. Oncoimmunology. 2018;7:e1502905.
20. Verdegaal EME, Santegoets SJ, Welters MJP, de Bruin L, Visser M, van der Minne CE, de Kok PM, Loof NM, Boekestijn S, Roozen I, Westra IM, Meij P, Van der Burg SH, Kroep JR. Timed adoptive T cell transfer during chemotherapy in patients with recurrent platinum-sensitive epithelial ovarian cancer. J Immunother Cancer. 2023;11(11):e007697.
21. Stevanovic S, Draper LM, Langhan MM, Campbell TE, Kwong ML, Wunderlich JR, Dudley ME, Yang JC, Sherry RM, Kammula US, et al. Complete regression of metastatic cervical cancer after treatment with human papillomavirus-targeted tumor-infiltrating T cells. J Clin Oncol. 2015;33:1543–50.
22. Huang H, Nie CP, Liu XF, Song B, Yue JH, Xu JX, He J, Li K, Feng YL, Wan T, Zheng M, Zhang YN, Ye WJ, Li JD, Li YF, Li JY, Cao XP, Liu ZM, Zhang XS, Liu Q, Zhang X, Liu JH, Li J. Phase I study of adjuvant immunotherapy with autologous tumor-infiltrating lymphocytes in locally advanced cervical cancer. J Clin Invest. 2022;132(15):e157726.
23. Slovin S, Carissimo A, Panariello F, Grimaldi A, Bouche V, Gambardella G, Cacchiarelli D. Single-Cell RNA sequencing analysis: a step-by-step overview. Methods Mol Biol. 2021;2284:343–65.
24. Zhang T, Wu Z, Li L, Ren J, Zhang Z, Wang G. CPPLS-MLP: a method for constructing cell-cell communication networks and identifying related highly variable genes based on single-cell sequencing and spatial transcriptomics data. Brief Bioinform. 2024;25(3):bbae198.
25. Alarcon B, Mestre D, Martinez-Martin N. The immunological synapse: a cause or consequence of T-cell receptor triggering? Immunology. 2011;133:420–5.
26. Tedder TF. CD19: a promising B cell target for rheumatoid arthritis. Nat Rev Rheumatol. 2009;5:572–7.
27. Lanier LL. Natural killer cell receptor signaling. Curr Opin Immunol. 2003;15:308–14.
28. Feng H, Qiu L, Shi Z, Sheng Y, Zhao P, Zhou D, Li F, Yu H, You Y, Wang H, et al. Modulation of intracellular kinase signaling to improve TIL stemness and function for adoptive cell therapy. Cancer Med. 2023;12:3313–27.
29. Kuncman L, Orzechowska M, Milecki T, Kucharz J, Fijuth J. High FLT3 expression increases immune-cell infiltration in the tumor microenvironment and correlates with prolonged disease-free survival in patients with non-small cell lung cancer. Mol Oncol. 2024;18:1316–26.
30. Takahashi S. Downstream molecular pathways of FLT3 in the pathogenesis of acute myeloid leukemia: biology and therapeutic implications. J Hematol Oncol. 2011;4:1–10.
31. Porta C, Paglino C, Mosca A. Targeting PI3K/Akt/mTOR Signaling in Cancer. Front Oncol. 2014;4:64.
32. Mohite R, Doshi G. Elucidation of the Role of the Epigenetic Regulatory Mechanisms of PI3K/Akt/mTOR Signaling Pathway in Human Malignancies. Curr Cancer Drug Targets. 2024;24:231–44.
33. Leiphrakpam PD, Are C. PI3K/Akt/mTOR Signaling Pathway as a Target for Colorectal Cancer Treatment. Int J Mol Sci. 2024;25:3178.
34. Bahrami A, Hasanzadeh M, Hassanian SM, ShahidSales S, Ghayour-Mobarhan M, Ferns GA, Avan A. The potential value of the PI3K/Akt/mTOR signaling pathway for assessing prognosis in cervical cancer and as a target for therapy. J Cell Biochem. 2017;118:4163–9.
35. Dong P, Konno Y, Watari H, Hosaka M, Noguchi M, Sakuragi N. The impact of microRNA-mediated PI3K/AKT signaling on epithelial-mesenchymal transition and cancer stemness in endometrial cancer. J Transl Med. 2014;12:231.
36. Yip PY. Phosphatidylinositol 3-kinase-AKT-mammalian target of rapamycin (PI3K-Akt-mTOR) signaling pathway in non-small cell lung cancer. Transl Lung Cancer Res. 2015;4:165–76.
37. Kryczek I, Zou L, Rodriguez P, Zhu G, Wei S, Mottram P, Brumlik M, Cheng P, Curiel T, Myers L, et al. B7–H4 expression identifies a novel suppressive macrophage population in human ovarian carcinoma. J Exp Med. 2006;203:871–81.
38. Zhang A, Fan T, Liu Y, Yu G, Li C, Jiang Z. Regulatory T cells in immune checkpoint blockade antitumor therapy. Mol Cancer. 2024;23:251.
39. Truxova I, Cibula D, Spisek R, Fucikova J. Targeting tumor-associated macrophages for successful immunotherapy of ovarian carcinoma. J Immunother Cancer. 2023;11(2):e005968.
40. Shen X, Wang C, Li M, Wang S, Zhao Y, Liu Z, Zhu G. Identification of CD8+ T cell infiltration-related genes and their prognostic values in cervical cancer. Front Oncol. 2022;12:1031643.
41. Li L, Ma Y, Liu S, Zhang J, Xu XY. Interleukin 10 promotes immune response by increasing the survival of activated CD8(+) T cells in human papillomavirus 16-infected cervical cancer. Tumour Biol. 2016;37:16093-101.
42. Huang H, Pan Y, Mai Q, Zhang C, Du Q, Liao Y, Qin S, Chen Y, Huang J, Li J, Liu T, Zou Q, Zhou Y, Yuan L, Wang W, Liang Y, Pan CY, Liu J, Yao S. Targeting CDCP1 boost CD8+ T cells-mediated cytotoxicity in cervical cancer via the JAK/STAT signaling pathway. J Immunother Cancer. 2024;12(10):e009416.

43. Gao W, Yuan H, Yin S, Deng R, Ji Z. Identification of three subtypes of ovarian cancer and construction of prognostic models based on immune-related genes. J Ovarian Res. 2024;17:208.
44. Balan D, Kampan NC, Plebanski M, Abd Aziz NH. Unlocking ovarian cancer heterogeneity: advancing immunotherapy through single-cell transcriptomics. Front Oncol. 2024;14:1388663.
45. Kennedy A, Patel S, Ramanathan M, Gerber J, Cerny J. Midostaurin for FLT3-mutated AML: a real-world analysis of effectiveness and infection risk at a single center. Ann Hematol. 2024;103:1031–3.
46. Zhao J, Song Y, Liu D. Gilteritinib: a novel FLT3 inhibitor for acute myeloid leukemia. Biomark Res. 2019;7:19.
47. Rajakumaraswamy N , Dauki A ,Michelle KuhneTorsten TroweWinnie WengKai-Wen LinEmon ElboudjwarejBrian CarrAngela WorthAnshu VashishthaChristian SchwabeAhmed Othman.380GS-3583, a novel FLT3 agonist Fc fusion protein, expands conventional dendritic cells in healthy volunteers. J Immunother Cancer. 2021;9(Suppl 3):413-4.
48. Tolcher AW, Brody JD, Rajakumaraswamy N, Kuhne M, Trowe T, Dauki AM, Pai S, Han L, Lin KW, Petrarca M, Kummar S. Phase I Study of GS-3583, an FMS-like Tyrosine Kinase 3 Agonist Fc Fusion Protein, in Patients with Advanced Solid Tumors. Clin Cancer Res. 2024;30:2954–63.
49. Dong HP, Li Y, Tang Z, Wang P, Zhong B, Chu Q, Lin D. Combined targeting of CCL7 and Flt3L to promote the expansion and infiltration of cDC1s in tumors enhances T-cell activation and anti-PD-1 therapy effectiveness in NSCLC. Cell Mol Immunol. 2023;20:850–3.
50. Leifheit ME, Johnson G, Kuzel TM, Schneider JR, Barker E, Yun HD, Ustun C, Goldufsky JW, Gupta K, Marzo AL. Enhancing Therapeutic Efficacy of FLT3 Inhibitors with Combination Therapy for Treatment of Acute Myeloid Leukemia. Int J Mol Sci. 2024;25(17):9448.

Publisher's Note

Springer Nature remains neutral with regard to jurisdictional claims in published maps and institutional affiliations.